

Truncation of Kir6.2 produces ATP-sensitive K⁺ channels in the absence of the sulphonylurea receptor

Stephen J. Tucker, Fiona M. Gribble, Chao Zhao, Stefan Trapp & Frances M. Ashcroft

University Laboratory of Physiology, Parks Road, Oxford OX1 3PT, UK

ATP-sensitive potassium channels (K-ATP channels) couple cell metabolism to electrical activity and are important in the physiology and pathophysiology of many tissues¹. In pancreatic β -cells, K-ATP channels link changes in blood glucose concentration to insulin secretion². They are also the target for clinically important drugs such as sulphonylureas, which stimulate secretion, and the K⁺ channel opener diazoxide, which inhibits insulin release^{3,4}. Metabolic regulation of K-ATP channels is mediated by changes in intracellular ATP and Mg-ADP levels, which inhibit and activate the channel, respectively². The β -cell K-ATP channel is a complex of two proteins^{5,6}: an inward-rectifier K⁺ channel subunit, Kir6.2, and the sulphonylurea receptor, SUR1. We show here that the primary site at which ATP acts to mediate K-ATP channel inhibition is located on Kir6.2, and that SUR1 is required for sensitivity to sulphonylureas and diazoxide and for activation by Mg-ADP.

There is accumulating evidence that Kir6.2 acts as the pore-forming subunit of the K-ATP channel, whereas SUR1 acts as a regulator of K-ATP channel activity, conferring sensitivity to sulphonylureas, diazoxide and Mg-ADP⁷⁻¹¹. The mechanism by which ATP inhibits the channel remains unknown and there has been considerable debate about whether the inhibitory ATP-binding site is located on Kir6.2 or SUR1. The facts that most Kir channels do not show marked sensitivity to ATP and that SUR1 possesses two nucleotide-binding domains (NBDs), whereas Kir6.2 has no obvious consensus sites for ATP binding, favour the idea that

SUR1 confers ATP sensitivity on Kir6.2; however, several findings argue against this idea. First, the sensitivity of native K-ATP currents to tolbutamide, diazoxide and Mg-ADP declines following patch excision, whereas the ability of ATP to block the channel remains unimpaired². Likewise, mild proteolysis of the inner membrane surface abolishes the sulphonylurea and Mg-ADP sensitivity of native K-ATP channels, but only slightly reduces their ATP sensitivity¹². Both these results suggest that Kir6.2 may functionally dissociate from SUR1 yet still retain sensitivity to ATP. The problem of which K-ATP channel subunit possesses the ATP-inhibitory site has been difficult to address because, unlike most other Kir channels, Kir6.2 does not express functional channels alone, but only when coexpressed with a sulphonylurea receptor (SUR1 or SUR2; refs 5, 6, 8). The reason for this is unclear. Although Kir6.2 is stably expressed in the absence of SUR1 (ref. 13), it may not reach the cell surface. An alternative idea is that Kir6.2 is present in the plasma membrane but in an inactivate state. As the amino terminus of voltage-gated K⁺ channels acts as a blocking particle, plugging the pore and inactivating the channel¹⁴, we reasoned that the same might be true for Kir6.2. We therefore tested the effects of deleting the distal parts of the amino or carboxy terminus of Kir6.2.

As previously reported¹³, large whole-cell currents can be recorded in response to metabolic inhibition from *Xenopus* oocytes conjoined with mRNAs encoding wild-type Kir6.2 and SUR1, but not from oocytes injected with wild-type Kir6.2 mRNA alone (Fig. 1a, b). In contrast, significant currents were recorded from oocytes injected with mRNA encoding a truncated form of Kir6.2 in which either the last 26 (Kir6.2 Δ C26) or 36 (Kir6.2 Δ C36) amino acids of the C terminus had been deleted. These currents were further enhanced by metabolic inhibition (Fig. 1a, b). This suggests that Kir6.2 Δ C26 and Kir6.2 Δ C36 are not only capable of independent expression but are also intrinsically sensitive to metabolically induced changes in cytosolic nucleotide levels.

To explore this possibility, we recorded macroscopic currents from giant inside-out patches excised from *Xenopus* oocytes expressing either wild-type Kir6.2, or Kir6.2 with N- or C-terminal deletions of different lengths. A marked increase in current was observed when patches were excised into nucleotide-free solution from oocytes expressing either Kir6.2 Δ C26 or Kir6.2 Δ C36 (Fig. 1c). This reflects the relief of the blocking action of ATP present in the

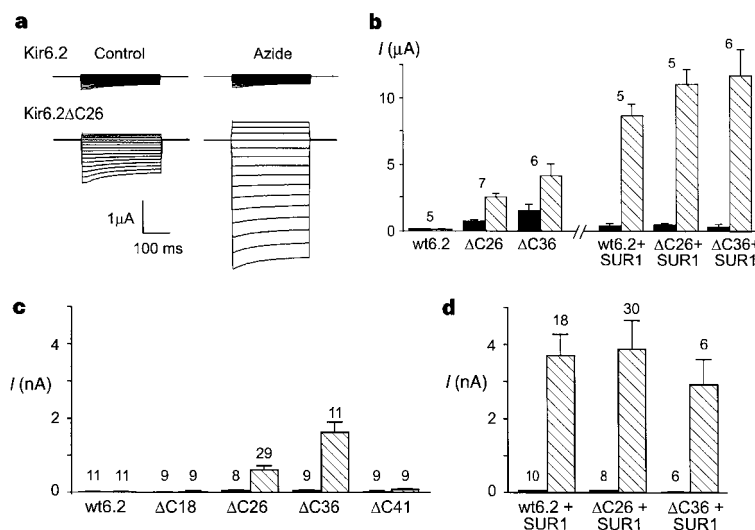


Figure 1 a, Whole-cell currents recorded from an oocyte injected with mRNA encoding wild-type (wt) Kir6.2 or Kir6.2 Δ C26 in response to a series of voltage steps from -120 to +20 mV before and 15 min after exposure to 3 mM azide. **b**, Mean whole-cell currents recorded at -100 mV before (filled bars) and 15 min after (hatched bars) exposure to 3 mM azide from oocytes injected with mRNA encoding wtKir6.2, Kir6.2 Δ C26, Kir6.2 Δ C36, wtKir6.2 + SUR1 (1:1 ratio),

Kir6.2 Δ C26 + SUR1 (1:1 ratio) or Kir6.2 Δ C36 + SUR1 (1:50 ratio). The number of oocytes is given above the bars. **c, d**, Mean macroscopic current amplitudes at -100 mV before (filled bars) and after (hatched bars) patch excision from oocytes injected with the mRNAs indicated. The number of patches is given above the bars.

oocyte cytoplasm. No increase in current on patch excision was observed with oocytes injected with wild-type Kir6.2 or when 14 residues were deleted from the N terminus of Kir6.2 ($n = 9$), and only a very small increase (<100 pA) was detected when either the last 18 residues (Kir6.2 Δ C18) or 41 residues (Kir6.2 Δ C41) of Kir6.2 were deleted from the C terminus (Fig. 1c). These results indicate that the last 18, or possibly 26, amino acids of Kir6.2 can prevent its independent functional expression. Coexpression of SUR1 enabled wild-type Kir6.2 to be expressed and also enhanced both Kir6.2 Δ C26 and Kir6.2 Δ C36 currents (Fig. 1d).

It is unclear why deletion of the C terminus of Kir6.2 should allow functional expression of the protein. One possibility is that the C terminus inhibits channel activity by blocking the pore. If so, then coupling of SUR1 to Kir6.2 might prevent the action of this blocking particle and so permit channel function. Alternatively, the C terminus might interact with other proteins that prevent either functional activity or surface expression of Kir6.2, effects that would be reversed by SUR1. The ability to express the truncated form of

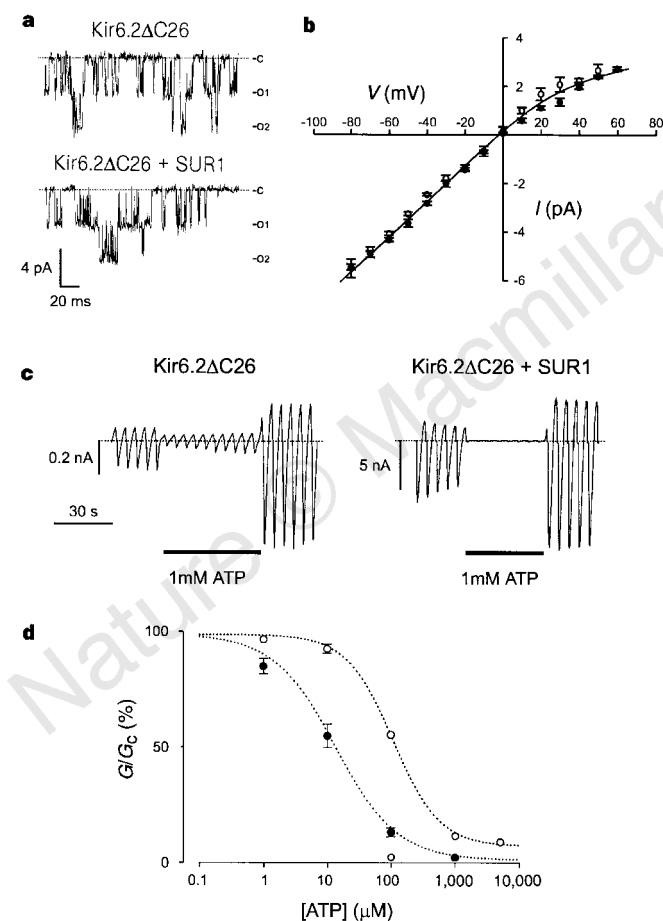


Figure 2 a, Single-channel currents recorded at -60 mV from an inside-out patch excised from an oocyte injected with mRNA encoding Kir6.2 Δ C26, or Kir6.2 Δ C26 + SUR1. **b**, Mean single-channel current–voltage relations recorded for Kir6.2 Δ C26 (circles) or Kir6.2 Δ C26 + SUR1 (filled circles). **c**, Macroscopic currents recorded from 2 different inside-out patches in response to a series of voltage ramps from -110 to $+100$ mV. Oocytes were injected with mRNAs encoding Kir6.2 Δ C26 or Kir6.2 Δ C26 + SUR1. 1 mM ATP was added to the internal solution as indicated by the bar. **d**, Mean ATP dose–response relationships for Kir6.2 Δ C26 currents (open circles; $n = 7$) and Kir6.2 Δ C26/SUR1 currents (filled circles; $n = 6$). Test solutions were alternated with control solutions and the slope conductance (G) is expressed as a percentage of the mean (G_c) of that in the control solution before and after exposure to ATP. Conductance was measured between -20 and -100 mV and is the mean of 5 voltage ramps. The lines are the best fits of the data to the Hill equation using the mean values for K_i and h given in the text.

Kir6.2 independently of SUR1 allowed us to investigate which properties of the K-ATP channel are intrinsic to Kir6.2 and which are endowed by SUR1.

Figure 2a, b shows single-channel currents and mean single-channel current–voltage relations recorded from inside-out patches excised from oocytes expressing Kir6.2 Δ C26 or Kir6.2 Δ C26 plus SUR1. The single-channel conductance, measured between -20 and -80 mV, was 69 ± 2 pS ($n = 4$) for Kir6.2 Δ C26 and 73 ± 2 pS ($n = 5$) for Kir6.2 Δ C26 plus SUR1. Thus, as SUR1 does not modify the single-channel conductance, it probably does not contribute to the main part of the permeation pathway. The single-channel conductance of Kir6.2 Δ C36 was 75 ± 2 pS ($n = 5$). None of these values are significantly different from those of wild-type Kir6.2/SUR1 currents (70 – 76 pS; refs 5, 6) or native K-ATP currents (50 – 80 pS; ref. 2), indicating that deletion of the C terminus does not alter the single-channel conductance.

Application of ATP to the inner membrane surface markedly inhibited both Kir6.2 Δ C26 and Kir6.2 Δ C36 currents (Fig. 2c, d), with half-maximal block (K_i) at 106 ± 4 μ M ($n = 7$) and 128 ± 5 μ M ($n = 6$), respectively. This suggests the Kir6.2 subunit possesses an intrinsic ATP-inhibitory site. The Hill coefficient (h) was 1.2 ± 0.1 ($n = 7$) for Kir6.2 Δ C26 and 1.0 ± 0.1 ($n = 6$) for Kir6.2 Δ C36. Its value is close to unity, which indicates that only a single ATP molecule needs to bind to close the channel. In β -cells, ATP inhibition does not require hydrolysis of the nucleotide². This was also the case for Kir6.2 Δ C36 currents as ATP-inhibition was unaffected by Mg^{2+} removal: 100 μ M ATP blocked the slope conductance by $44 \pm 2\%$ ($n = 9$) in the presence of 1.4 mM Mg^{2+} and by $42 \pm 2\%$ ($n = 6$) in Mg^{2+} -free solution. Coexpression of SUR1 with Kir6.2 Δ C26 increased the potency of ATP inhibition (Fig. 2c, d) to that found for wild-type K-ATP channels: $K_i = 13.4 \pm 0.3$ μ M ($n = 8$) for Kir6.2 Δ C26/SUR1 and 10 – 28 μ M for wild-type Kir6.2/SUR1 currents^{5,15}. Likewise, the K_i for ATP inhibition of Kir6.2 Δ C36/SUR1 currents (24.6 ± 2.4 μ M; $n = 5$) was lower than that of Kir6.2 Δ C36 currents (128 μ M).

To exclude the possibility that Kir6.2 Δ C36 or Kir6.2 Δ C26 couple to an endogenous protein in the *Xenopus* oocyte that makes it ATP-sensitive, we also examined whether truncated Kir6.2 expresses ATP-sensitive currents in mammalian cells. Whole-cell currents recorded from HEK293 cells transfected with Kir6.2 Δ C36 increased

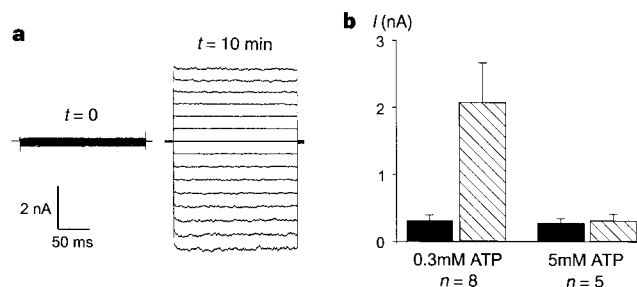


Figure 3 a, Whole-cell currents recorded from an HEK293 cell transfected with cDNA encoding Kir6.2 Δ C36 in response to a series of voltage steps from -110 to $+30$ mV, immediately after forming the whole-cell configuration and ~ 10 min later. The pipette contained 0.3 mM ATP. **b**, Mean whole-cell current amplitudes recorded from HEK293 cells transfected with cDNA encoding Kir6.2 Δ C36 immediately after forming the whole-cell configuration (black bars) and ~ 10 min later (hatched bars). Cells were dialysed with the ATP concentrations indicated.

with time following establishment of the whole-cell configuration when dialysed intracellularly with 0.3 mM ATP (Fig. 3). This increase in current results from the washout of endogenous ATP from the cell as it was not evident when cells were dialysed with 5 mM ATP. Similar results were found for Kir6.2ΔC26 currents (not shown) and wild-type Kir6.2/SUR1 currents⁶. Other K⁺ channels that require an additional subunit for expression in oocytes (for example, Kir3.1 and Isk) are not expressed by themselves in mammalian cells, but in *Xenopus* oocytes they give small currents that are limited in size by the amount of endogenous subunit present^{15,16}. This is not the case for Kir6.2ΔC26 and Kir6.2ΔC36, strongly suggesting that they are capable of independent expression and so are intrinsically ATP sensitive.

As the free ATP molecule carries four negative charges, it seems likely that a positively charged residue may form part of the ATP-binding site. We found that neutralization of the lysine residue at position 185 to glutamine (Kir6.2ΔC26-K185Q) substantially decreased the channel sensitivity to ATP (Fig. 4): K_i was 4.2 ± 0.2 mM ($n = 6$) for Kir6.2ΔC26-K185Q currents compared with 106 ± 4 μM ($n = 7$) for Kir6.2ΔC26 currents. The Hill coefficient was unaffected, being 1.2 ± 0.1 for both Kir6.2ΔC26-K185Q ($n = 6$) and Kir6.2ΔC26 ($n = 7$) currents. These data provide further support for the idea that ATP interacts directly with Kir6.2 to mediate channel inhibition. They also suggest that Lys 185 is involved in this inhibition, either by forming part of the ATP-binding site itself or by constituting part of the transduction mechanism by which binding of ATP to a site elsewhere effects channel closure.

Figure 2d shows that although the primary site at which ATP inhibits the K-ATP channel resides on Kir6.2, the presence of SUR1 can enhance the blocking action of the nucleotide (from ~100 to ~10 μM). Furthermore, when SUR1 was coexpressed with Kir6.2ΔC26-K185Q, the ATP sensitivity was also slightly greater than that found in the absence of the sulphonylurea receptor ($K_i = 2.3 \pm 0.1$ mM; $n = 6$, $P < 0.001$). This enhancement need not imply that ATP interacts with a second inhibitory site on SUR1: for example, the sulphonylurea receptor may simply facilitate access of ATP to its inhibitory site on Kir6.2. One reason it has been postulated that the inhibitory binding site for ATP lies on SUR1 is that the K_i for ATP inhibition of Kir6.2/SUR1 currents is ~10 μM, whereas that for Kir6.2/SUR2 currents is ~100 μM (refs 5, 8). Our results suggest this difference may be because SUR1, but not SUR2, enhances the ATP sensitivity of Kir6.2.

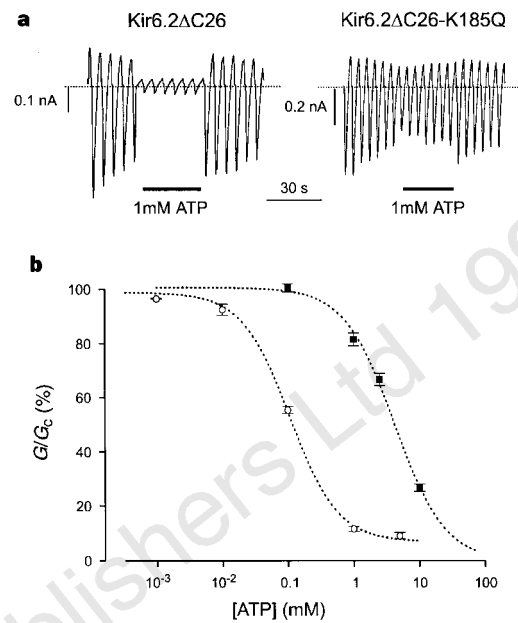


Figure 4 a, Macroscopic currents recorded from 2 different inside-out patches in response to a series of voltage ramps from -110 to +100 mV. Oocytes were injected with mRNAs encoding Kir6.2ΔC26 or Kir6.2ΔC26-K185Q. 1 mM ATP was added to the internal solution as indicated by the bar. **b**, Mean ATP dose-response relationships for Kir6.2ΔC26 currents (open circles; $n = 7$) and Kir6.2ΔC26-K185Q currents (filled squares; $n = 6$). Test solutions were alternated with control solutions and the slope conductance (G) is expressed as a percentage of the mean (G_c) of that obtained in control solution before and after exposure to ATP. Conductance was measured between -20 and -100 mV and is the mean of 5 voltage ramps. The lines are the best fits of the data to the Hill equation using the mean values for K_i and the Hill coefficient given in the text.

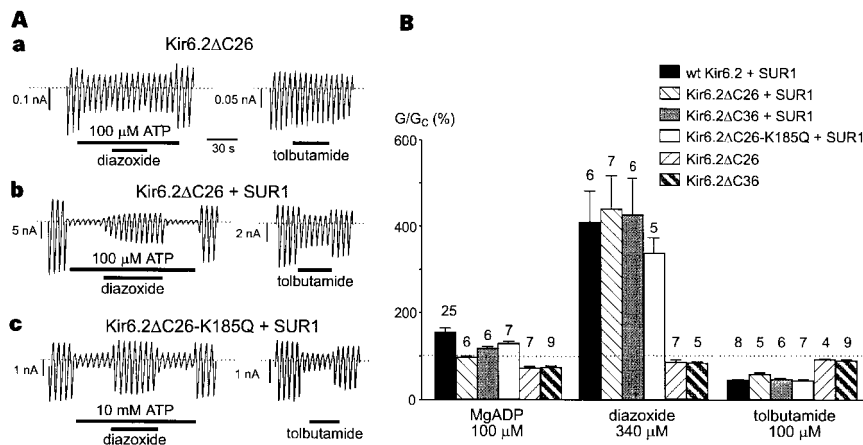


Figure 5 A, Macroscopic currents recorded from inside-out patches in response to a series of voltage ramps from -110 to +100 mV. Oocytes were injected with mRNAs encoding Kir6.2ΔC26 (**a**), Kir6.2ΔC26 + SUR1 (1:1 ratio) (**b**), or Kir6.2ΔC26-K185Q + SUR1 (1:50 ratio) (**c**). 100 μM Mg-ATP, 340 μM diazoxide or 100 μM tolbutamide was added to the internal solution, as indicated by the bars. **B**, Mean macroscopic slope conductance recorded in the presence of 100 μM

Mg-ADP or 100 μM tolbutamide, expressed as a percentage of the slope conductance in control solution (no additions). Diazoxide (340 μM) was added in the presence of 100 μM Mg-1-ATP or 10 mM Mg-ATP (Kir6.2ΔC26-K185Q + SUR1, only) and is expressed as a percentage of the current amplitude in Mg-ATP solution. The dashed line indicates the current level in the absence of the test compound. The number of patches is given above the bars.

The finding that the ATP-inhibitory site is located on Kir6.2, rather than on the sulphonylurea receptor, is consistent with the facts that SUR2B forms an ATP-sensitive K⁺ channel with Kir6.2 but an ATP-insensitive K⁺ channel with Kir6.1 (ref. 17), and that other Kir subunits such as Kir1.1b (ROMK2) and Kir2.3, which are expressed independently, are blocked by high concentrations of ATP (~5 mM; refs 18, 19). Furthermore, the reported mutations within the NBDs of SUR1 do not reduce ATP sensitivity^{10,11}. It is perhaps not surprising that the NBDs of SUR1 do not act as the primary site of ATP block because in other ABC transporters the primary role of these domains is to hydrolyse Mg-ATP²⁰, whereas the β-cell K-ATP channel is blocked by the free base ATP^{4–7} (refs 1, 2).

As found for the native and wild-type K-ATP currents^{2,11}, both Kir6.2ΔC26 (Fig. 2) and Kir6.2ΔC36 currents ran down with time in excised patches, and were refreshed following exposure to Mg-ATP. This indicates that both these properties are intrinsic to Kir6.2 rather than to SUR1.

Both native β-cell K-ATP and wild-type Kir6.2/SUR1 currents are blocked by tolbutamide and potentiated by Mg-ADP and diazoxide^{1,5,6}; the stimulatory action of the latter is dependent upon the presence of intracellular hydrolysable nucleotides^{1,2}. Figure 5A, a shows that both tolbutamide and diazoxide (in the presence of 100 μM ATP) were without effect on Kir6.2ΔC26 currents at concentrations that markedly alter wild-type Kir6.2/SUR1 currents¹³. Furthermore, Mg-ADP blocked Kir6.2ΔC26 currents (Fig. 5B). This result is not unexpected, because the NBDs of SUR1 confer Mg-ADP activation on the K-ATP channel and in the absence of this activation an inhibitory effect of the nucleotide is unmasked^{10,11}. It also suggests that, like ATP, the inhibitory effect of ADP is intrinsic to Kir6.2. Metabolic inhibition caused greater activation of whole-cell Kir6.2ΔC26/SUR1 (or Kir6.2ΔC36/SUR1) currents than whole-cell Kir6.2ΔC26 (or Kir6.2ΔC36) currents (Fig. 1b). This may reflect the potentiatory action of Mg-ADP conferred by SUR1 and supports the view that the stimulatory effect of Mg-ADP is important in coupling metabolism to K-ATP channel activity^{1,2,10,11}.

Coexpression of Kir6.2ΔC26 with SUR1 restored the efficacy of diazoxide to that found for wild-type currents and almost fully restored the effects of tolbutamide and Mg-ADP (Fig. 5A, b and B). These data confirm that SUR1 makes the K-ATP channel sensitive to sulphonylureas, diazoxide and the potentiatory action of Mg-ADP [7–11]. Similar results were found for Kir6.2ΔC36, providing that an excess of SUR1 mRNA was injected (Fig. 5B); when equivalent amounts of mRNAs were injected, no coupling was observed. Likewise, coexpression of Kir6.2ΔC26-K185Q with SUR1 resulted in currents that were inhibited by tolbutamide and activated by Mg-ADP and diazoxide (Fig. 5A, c and B). This indicates that although K185 is involved in channel closure induced by ATP, it is not required for inhibition by sulphonylureas.

In conclusion, we have shown that the last 18 (or 26) amino acids of Kir6.2 prevent its independent functional expression. This effect is reversed by SUR1. Our results provide evidence that Kir6.2 acts as the pore of the K-ATP channel complex and that SUR1 endows Kir6.2 with sensitivity to sulphonylureas, diazoxide and Mg-ADP. Importantly, they also indicate that the primary site at which ATP interacts to mediate channel inhibition is located on Kir6.2 and not on SUR1, as previously suggested. However, although the ATP-inhibitory site lies on Kir6.2, SUR1 enhances the sensitivity of Kir6.2 to ATP (from $K_i \approx 100 \mu\text{M}$ to $K_i \approx 10 \mu\text{M}$). Our results are likely to be applicable to K-ATP channels in brain, cardiac and skeletal muscle, where Kir6.2 is also thought to act as the pore-forming subunit^{5,6,8,21}. Finally, that Kir6.2ΔC26 can be expressed independently makes it a useful tool for determining whether drugs that act on K-ATP channels do so by interacting with Kir6.2 or with SUR1, and for examining the functional interaction between Kir6.2 and SUR1. □

Methods

Molecular biology. C-terminal deletions of mouse Kir6.2 (Genbank D50581) were made by introduction of a stop codon at the appropriate residues by site-directed mutagenesis. The N-terminal deletion was similarly constructed by removal of the original start codon and replacement of the leucine residue at position 14 with an initiator methionine. Synthesis of mRNA encoding wild-type and mutant mouse Kir6.2 and wild-type rat SUR1 (Genbank, L40624) was performed as described¹³.

Electrophysiology. *Xenopus* oocytes were defolliculated and injected with ~2 ng mRNA encoding either full-length or truncated Kir6.2. In coexpression experiments, ~2 ng wild-type (wt) Kir6.2, ~2 ng Kir6.2ΔC26 or ~0.04 ng Kir6.2ΔC36 mRNA was injected with 2 ng SUR1 mRNA (giving a 1:1 or 1:50 ratio). The final injection volume was ~50 nl per oocyte. Isolated oocytes were maintained in tissue culture¹³ and studied 1–4 days after injection. Whole-cell currents were measured at 18–24 °C using a standard 2-electrode voltage clamp¹³ in (mM): 90 KCl, 1 MgCl₂, 1.8 CaCl₂, 5 HEPES (to pH 7.4 with KOH). The holding potential was –10 mV. Currents were filtered at 1 kHz, digitized at 4 kHz and measured 280–295 ms after the start of the voltage pulse. Macroscopic (or single-channel) currents were recorded from giant (or normal) excised inside-out patches at a holding potential of 0 mV and at 20–24 °C (refs 11, 22). The pipette solution contained (mM): 140 KCl, 1.2 MgCl₂, 2.6 CaCl₂, 10 HEPES (pH 7.4 with KOH) and the internal (bath) solution contained (mM): 110 KCl, 1.44 MgCl₂, 30 KOH, 10 EGTA, 10 HEPES (pH 7.2 with KOH), plus nucleotides as indicated. The Mg²⁺-free solution contained (mM): 110 KCl, 30 KOH, 2.6 CaCl₂, 10 EDTA, 10 HEPES (pH 7.2 with KOH). Macroscopic currents were recorded in response to 4-s voltage ramps from –110 to +100 mV with an EPC7 amplifier (List Elektronik, Darmstadt, Germany), filtered at 0.2 kHz and sampled at 0.5 kHz. The slope conductance was measured by fitting a straight line to the data between –20 and –100 mV: the average of 5 consecutive ramps was calculated in each solution. Single-channel currents were filtered at 1 kHz and sampled at 3 kHz.

HEK293 cells were transiently transfected with the pcDNA3 vector (Invitrogen) containing the coding sequence of wild-type or mutant Kir6.2 using lipofectamine (GibcoBRL)⁶. Whole-cell currents were studied 48–72 h after transfection. The pipette solution contained (mM): 107 KCl, 1.2 MgCl₂, 1 CaCl₂, 10 EGTA, 5 HEPES (pH 7.2 with KOH); total K⁺ ~140 mM and either 0.3 or 5 mM ATP. The bath solution contained (mM): 40 KCl, 100 NaCl, 2.6 CaCl₂, 1.2 MgCl₂, 5 HEPES (pH 7.4). The holding potential was –30 mV.

Data analysis. All data is given as mean ± s.e.m. The symbols in the figures indicate the mean and the vertical bars one s.e.m. (where this is larger than the symbol). ATP dose–response relationships were fitted to the Hill equation: $G/G_c = O + (100 - O)/(1 + ([ATP]/K_i)^h)$, where [ATP] is the ATP concentration, K_i is the ATP concentration at which inhibition is half maximal, h is the slope factor (Hill coefficient) and O is the background current (not blocked by ATP). Statistical significance was tested using Student's *t*-test.

Received 14 January; accepted 21 March 1997.

- Ashcroft, F. M. & Ashcroft, S. J. H. Properties and functions of ATP-sensitive K-channels. *Cell. Signal* **2**, 197–214 (1990).
- Ashcroft, F. M. & Rorsman, P. Electrophysiology of the pancreatic β-cell. *Prog. Biophys. Mol. Biol.* **54**, 87–143 (1989).
- Ashcroft, F. M. & Ashcroft, S. J. H. The sulphonylurea receptor. *Biochim. Biophys. Acta* **1175**, 45–59 (1992).
- Dunne, M. J., Harding, E., Jaggar, J. H., Ayton, B. J. & Squires, P. E. in *Frontiers of Insulin Secretion and Pancreatic β-Cell Research*. (eds Flatt, P. & Lenzen, S.) 153–59 (Smith Gordon, UK, 1993).
- Inagaki, N. et al. Reconstitution of IKATP: an inward rectifier subunit plus the sulphonylurea receptor. *Science* **270**, 1166–1169 (1995).
- Sakura, H., Ämmälä, C., Smith, P. A., Gribble, F. M. & Ashcroft, F. M. Cloning and functional expression of the cDNA encoding a novel ATP-sensitive potassium channel expressed in pancreatic β-cells, brain, heart and skeletal muscle. *FEBS Lett.* **377**, 338–344 (1995).
- Angular-Bryan, L. et al. Cloning of the β-cell high-affinity sulphonylurea receptor: a regulator of insulin secretion. *Science* **268**, 423–425 (1995).
- Inagaki, N. et al. A family of sulphonylurea receptors determines the properties of ATP-sensitive K⁺ channels. *Neuron* **16**, 1011–1017 (1996).
- Ämmälä, C., Moorhouse, A. & Ashcroft, F. M. The sulphonylurea receptor confers diazoxide sensitivity on the inwardly-rectifying K-channel, Kir6.1. *J. Physiol. (Lond.)* **494**, 709–714 (1996).
- Nichols, C. G. et al. Adenosine diphosphate as an intracellular regulator of insulin secretion. *Science* **272**, 1785–1787 (1996).
- Gribble, F. M., Tucker, S. J. & Ashcroft, F. M. The essential role of the Walker A motifs of SUR1 in K-ATP channel activation by MgADP and diazoxide. *EMBO J.* **16**, 1145–1152 (1997).
- Proks, P. & Ashcroft, F. M. Modification of K-ATP channels in pancreatic β-cells by trypsin. *Pflügers Arch.* **424**, 63–72 (1993).
- Gribble, F. M., Ashfield, R., Ämmälä, C. & Ashcroft, F. M. Properties of cloned ATP-sensitive K-currents expressed in *Xenopus* oocytes. *J. Physiol. (Lond.)* **498**, 87–98 (1997).
- Hoshi, T., Zagotta, W. N. & Aldrich, R. W. Biophysical and molecular mechanisms of Shaker potassium channel inactivation. *Science* **250**, 533–538 (1990).

15. Kravinsky, G. *et al.* The G-protein-gated atrial K⁺ channel I_{KACH} is a heteromultimer of two inwardly rectifying K⁺-channel proteins. *Nature* **374**, 135–141 (1995).
16. Sanguinetti, M. C. *et al.* Coassembly of K_vLQT1 and MinK (IsK) proteins to form cardiac I_{Ks} potassium channel. *Nature* **384**, 80–83 (1996).
17. Yamada, Y. M. *et al.* Sulphonylurea receptor 2B and Kir6.1 form a sulphonylurea-sensitive but ATP insensitive K⁺ channel. *J. Physiol. (Lond.)* **499**, 715–720 (1997).
18. McNicholas, C. M., Yang, Y., Gebeisch, G. & Hebert, S. C. Molecular site for nucleotide binding on an ATP-sensitive renal K⁺ channel (ROMK2). *Am. J. Physiol.* **271**, F275–F285 (1996).
19. Collins, A., German, M. S., Jan, Y. N., Jan, L. Y. & Zhao, B. A strongly inwardly rectifying K⁺ channel that is sensitive to ATP. *J. Neurosci.* **16**, 1–9 (1996).
20. Higgins, C. F. ABC transporters: from microorganisms to man. *Annu. Rev. Cell Biol.* **8**, 67–113 (1992).
21. Karschin, C., Ecke, C., Ahncroft, F. M. & Karschin, A. Overlapping tissue distribution of K_{ATP} channel-forming Kir6.2 subunit and the sulphonylurea receptor SUR1 in rodent brain. *FEBS Lett.* **401**, 59–64 (1996).
22. Hilgemann, D. W., Nicoll, D. A. & Phillipson, K. D. Charge movement during Na⁺ translocation by native and cloned Na⁺/Ca²⁺ exchanger. *Nature* **352**, 715–718 (1991).

Acknowledgements. We thank G. Bell for the gift of rat SUR1, and B. Fakler and P. Ruppersberg for discussion. We also thank the Wellcome Trust, the British Diabetic Association and the MRC for support. F.M.G. is an MRC Clinical Training Fellow. S.T. is supported by the Deutsche Forschungsgemeinschaft, and S.J.T. is a Wellcome Trust Fellow.

Correspondence and requests for materials should be addressed to F.M.A. (e-mail: frances.ashcroft@physiol.ox.ac.uk).

Quantification of latent tissue reservoirs and total body viral load in HIV-1 infection

Tae-Wook Chun*, Lucy Carruth*, Diana Finzi*, Xuefei Shen*, Joseph A. DiGiuseppe†, Harry Taylor*, Monika Hermankova*, Karen Chadwick‡, Joseph Margolick‡, Thomas C. Quinn*§, Yen-Hong Kuo||, Ronald Brookmeyer||, Martha A. Zeiger†, Patricia Barditch-Crovo* & Robert F. Siliciano*

Departments of *Medicine, †Pathology, and ‡Surgery, Johns Hopkins University School of Medicine, Baltimore, Maryland 21205, USA

Departments of ‡Molecular Microbiology and Immunology, and ||Biostatistics, Johns Hopkins University School of Hygiene and Public Health, Baltimore, Maryland 21205, USA

§ National Institute of Allergy and Infectious Diseases, National Institutes of Health, Bethesda, Maryland 20892, USA

The capacity of HIV-1 to establish latent infection of CD4⁺ T cells may allow viral persistence despite immune responses and antiretroviral therapy. Measurements of infectious virus^{1,2} and viral RNA^{3,4} in plasma and of infectious virus¹, viral DNA^{5–10} and viral messenger RNA species^{11–14} in infected cells all suggest that HIV-1 replication continues throughout the course of infection. Uncertainty remains over what fraction of CD4⁺ T cells are infected and whether there are latent reservoirs for the virus. We show here that during the asymptomatic phase of infection there is an extremely low total body load of latently infected resting CD4⁺ T cells with replication-competent integrated provirus (<10⁷ cells). The most prevalent form of HIV-1 DNA in resting and activated CD4⁺ T cells is a full-length, linear, unintegrated form that is not replication competent. The infection progresses even though at any given time in the lymphoid tissues integrated HIV-1 DNA is present in only a minute fraction of the susceptible populations, including resting and activated CD4⁺ T cells and macrophages.

The importance of latent reservoirs for HIV-1 is highlighted by studies of potent antiretroviral drugs that block new rounds of infection and produce a dramatic drop in plasma virus in two weeks. The rapid decline shows that virus production results largely from continuous rounds of virus infection of and replication in host cells with rapid turnover of free virus and virus-producing cells^{15–18}. Subsequently, however, plasma virus declines at a slower rate, presumably reflecting the turnover of long-term reservoirs of chronically or latently infected cells³⁰. Latent infection of CD4⁺ T cells may occur through two mechanisms, both of which are operative only in cells that are in a resting G₀ state. Partially or

completely reverse-transcribed HIV-1 DNA may be present in the cytoplasm of infected resting CD4⁺ T cells as a result of a block in reverse transcription or nuclear import and may constitute a labile, inducible reservoir^{6,19,20}. A second, more stable latent reservoir comprises resting CD4⁺ T cells with integrated provirus²¹. Little is known about the size, characteristics and functional significance of latent cellular reservoirs for HIV-1.

The latent reservoirs were studied in 14 asymptomatic, HIV-1-infected donors (CD4 counts 200–700 cells μl⁻¹; plasma RNA 1,400–116,000 copies ml⁻¹). Half of the donors were receiving antiretroviral therapy (nucleoside analogues). Because lymph nodes may represent an important site for viral replication^{9,10}, node biopsies were obtained. These showed follicular hyperplasia, follicular involution, and mixed patterns. Immunohistochemical staining for p24 antigen revealed diffuse follicular localization and rare productively infected cells with intense cytoplasmic staining. To determine the frequency of latently infected CD4⁺ T cells with integrated HIV-1 DNA, we isolated resting CD4⁺ T cells from lymph nodes and blood. Although the fraction of CD4⁺ T cells that were activated (HLA DR⁺) was higher in the lymph nodes than in blood (40 ± 13% versus 24 ± 9%), resting CD4⁺ T cells could be isolated from both sources with >99% purity. Resting cells did not release detectable virus. The frequency of resting CD4⁺ T cells with integrated HIV-1 DNA was measured using a quantitative version of an inverse polymerase chain reaction (PCR) assay²¹ that specifically detects integrated HIV-1 DNA by amplifying unique upstream host genomic sequences (Fig. 1a). Sequence analysis of the inverse PCR products revealed fusion of the 5' long terminal repeat (LTR) to cellular (non-HIV) sequences, with the expected loss of two bases from the HIV-1 genome at the junction²² and ligation of gag sequences to cellular DNA at the PstI site (Fig. 1b). The inverse PCR assay was carried out at a limiting dilution with a second nested amplification of an internal gag sequence. This approach compensates for the tendency of inverse PCR to give preferential amplification of small templates. For a control plasmid construct and for ACH-2 cells, which give inverse PCR products of 0.4 and 1.7 kilobases (kb), respectively, very strong ligase-dependent bands were seen even after dilution to the level of 3–5 copies in 30,000 cell equivalents of DNA (Fig. 1c). The signal extinguished upon dilution to 0.3–0.5 copies. Thus, for integration events giving inverse PCR bands of <2 kb, the assay can detect a single integration in 30,000 cell equivalents of human DNA. Because dilution series

Table 1 Virus load in activated CD4⁺ T cells

Donor*	CD4 ⁺ DR ⁺ T cells with integrated HIV† (per 10 ⁶ cells)	Upper bound for CD4 ⁺ DR ⁺ T cells with integrated HIV‡ (per 10 ⁶ cells)	Total body load of CD4 ⁺ DR ⁺ T cells with integrated HIV§
4	387	1,410	5.2 × 10 ⁷
5	101	410	1.8 × 10 ⁷
6	257	1,280	2.3 × 10 ⁷
8	172	542	2.5 × 10 ⁷
9	598	1,768	6.7 × 10 ⁷
10	345	1,132	5.9 × 10 ⁷
12	80	376	1.2 × 10 ⁷
Mean	224	–	3.1 × 10 ⁷

* Calculations were made for donors whose lymph node samples had clearly measurable integrated HIV-1 DNA in both the unfractionated and purified resting CD4⁺ T cell populations. In the remaining donors, integrated HIV-1 DNA was below the limit of detection in the unfractionated populations, suggesting an even lower total body load of activated CD4⁺ T cells with integrated HIV-1 DNA.

† Determined by subtraction using values of integrated HIV-1 DNA in unfractionated and purified resting CD4⁺ T cells and the frequencies of resting and activated CD4⁺ T cells in the lymph nodes. Calculations are based on the assumption that after depletion of adherent cells, all integrated HIV-1 in lymph node mononuclear cells is either in resting or activated CD4⁺ T cells.

‡ Because these estimates are based on the subtraction of two experimentally derived values, each with its own variance, an upper bound on the frequency of activated CD4⁺ T cells with integrated HIV-1 DNA was also determined as the calculated frequency +2s.e. Standard errors were determined using the rule of total probability from the variances for the frequencies of unfractionated and purified cells with integrated HIV-1 DNA. These variances were calculated from the confidence intervals given in ref. 29. The conservative assumption of independence was made.

§ Calculated using the fraction of CD4⁺DR⁺ cells among lymph node cells assuming a total body population of 10¹² lymphocytes.